Effects of load distribution exerting on coal pillars on the stress and energy distribution of the floor strata

***Jing-Xuan Yang*[1], *Chang You Liu*[1] *and* *Bin Yu*[2]**

A theoretical analysis was conducted to establish a mathematical model of stress calculation in floor strata when the coal pillars are under arbitrary linear loading. It was shown that the distribution forms of stress and energy were the same, but the effect of the uniform loading on stress and energy value was greater than the bilinear loading condition under the same peak loading and elevation position. Within a certain critical distance from the bottom of the pillar, the vertical stress and energy density were mainly affected by the overlying single pillar action, but were gradually affected by the interactions between the multiple pillars beyond this critical distance. The horizontal stress was more vulnerable to the interactions of the multiple pillars under different loading conditions; then a method of the segmented straightening of the actual loading curve for the coal pillars on the stress calculation was proposed.

Key words: *coal pillars, stress and energy, uniform loading, linear loading*

Introduction

The coal seams in China's central and western regions have rich reserves, and are characterized with the occurrence of close distance, and room and pillar mining as well as longwall mining leaving behind section protective coal pillars, so that a large number of coal pillars have been retained in the goaf areas. With the lower seam being mined, the coal pillars left behind in goaf areas in the overlying coal seam will affect the lower coal seam mining. This effect is particularly significant when the layer spacing between coal seams is very small. At present, in some regions in China's Inner Mongolia, coal mining operations in the majority of mines are below the room, and pillar mined goaf areas of the shallow-buried coal seams. Affected by the overlying goaf pillars, the roof of the working face fails irregularly, and the cyclic changes of the pressure are large (Yang JX et al., 2013). In the Datong mining region of China's Shanxi province, after the extraction of the overlying Jurassic coal seam, boundary and section pillars left behind in the goaf areas have similarly brought certain effects on the mining of the Carboniferous seam below. The measured results indicate that although the layer spacing is relatively large, i.e., 150 ~ 200 m, under the mining influence of the super-thick Carboniferous seam, when the failure of the overlying strata of super-thick coal seam is spread to the central areas affected by energy created in the floor strata by the coal pillars, the sudden release of concentrated elastic energy will lead to the occurrence of high rock pressure on the Carboniferous coal face below (Yu B, 2014). Therefore, the theoretical analysis of the pattern of theimpact of the coal pillars in the overlying coal goaf on the stress and energy distribution in the floor strata has practical significance. Due to the difficulty in theoretical analysis, the majority of current studies about the stress in floor strata are still limited to the discussion of uniform loading condition. For example, there is relevant research on the roof structure involving coal pillar issues, and the roof stability conditions under the pillar influence, failure mechanism and characteristics of roof pressure have been obtained (Meng D et al., 2007; Gong PL and Jin ZM, 2008; Yang JX et al., 2013; Hao HJ et al., 2004). Discussions about coal pillars left under buildings and about roadway stability under the impact of coal pillars have resulted in the standard of safety coal pillar sizes as well as the stability mechanisms of roadways (Liu BC and Shen HQ, 1988; Wang WJ and Hou CJ, 2003; Gong KY and Shan CJ, 2001; Tu SH et al., 2010; Gao MS et al., 2005). The pillar loading, which is subjected to overburden stress of the overlying strata, presents a variety of distribution patterns. This paper first presents the analytical solution of the stress in floor strata under arbitrary linear loading condition; then a comparative analysis was conducted on stress and energy distribution characteristics as well as the interactions between the coal pillars in the goaf areas under the conditions of the bilinear and uniform loading; finally, we provide a solution and calculation method of floor strata stress under arbitrary loading forms.

[1] *Jing-Xuan Yang, Chang You Liu,* China University of Mining & Technology, School of Mines, Key Laboratory of Deep Coal Resource Mining, Ministry of Education of China, Xuzhou, 221116, China, jxyangcumt@126.com
[2] *Bin Yu,* Datong Coal Mine Group Company, Datong, 037003, China

Theoretical model construction of the effects of coal pillars in goaf areas

Following the coal mining, the roof strata in the goaf areas subjected to complex movement and adjustment, eventually forming a stable arched structure. Coal pillars, left behind in the goaf areas as the arch foot have high concentrated stress, leading to a certain high-stress area in floor strata surrounding the coal pillars. However, the floor strata below the pillars bear loads from three directions due to restrictions in space, and floor strata, when bearing high stress, are generally still at the elastic load-bearing stage. In order to understand the extent of the affected areas by the high stress produced by coal pillars, as well as the interactions between pillars, a model of coal and rock load transfer under concentrated stress from coal pillars was constructed, as shown in Fig.1, where x -axis represents the down orientation, and y -axis the left orientation.

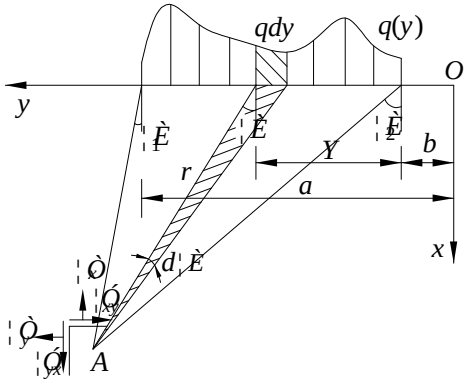

Fig. 1. A transfer model under the pillar stress condition (Xu ZL, 2006).

Based on the solution method of the stress in a semi-infinite body under concentrated force, the radial stress of floor strata under the effect of coal pillars' micro-unit body satisfies the following relationship:

$$d\sigma_r = -\frac{2q(y)dy}{\pi}\frac{\cos\theta}{r} \tag{1}$$

where σ_r is the rock radial stress, $q(y)$ the pillar loading, dy the width of the micro-unit body of the pillar, θ the vertical angle between the stress point A in floor strata below the pillar and the boundaries of the micro-unit body, r the radial distance between stress point A and micro-unit body.

As indicated in Fig.1, the following geometric relationship is established:

$$dy = \frac{r}{\cos\theta}d\theta \tag{2}$$

where $d\theta$ is the increments of the perpendicular angle formed between stress A and the two boundaries of the micro-unit body.

Based on the conversion between polar coordinates and Cartesian coordinates, the floor strata stress under arbitrary loading condition in the Cartesian coordinates obtained from integral is as follows:

$$\begin{cases} \sigma_x = -\dfrac{2}{\pi}\displaystyle\int_{\theta_1}^{\theta_2} q(y)\cos^2\theta d\theta \\ \sigma_y = -\dfrac{2}{\pi}\displaystyle\int_{\theta_1}^{\theta_2} q(y)\sin^2\theta d\theta \\ \tau_{xy} = -\dfrac{1}{\pi}\displaystyle\int_{\theta_1}^{\theta_2} q(y)\sin 2\theta d\theta \end{cases} \tag{3}$$

where σ_x, σ_y, and τ_{xy} are the vertical stress, horizontal stress and the shear stress component in Cartesian coordinates, respectively.

To facilitate the calculation, the floor strata stress when the coal pillar is under the arbitrary linear loading condition will be analyzed first. Assuming the form of the linear load borne by the coal pillar is as follows:

$$q(y) = \alpha y + \beta \tag{4}$$

where α is the loading coefficient and β the loading constant.

Based on the geometric relationship shown in Fig.1, and the triangle sine, the distance between the concentrated force of the micro-unit body and the right boundary of the pillar, as well as the distance between stress point A and pillar micro-unit body, are obtained, respectively, as follows:

$$\begin{cases} Y = \dfrac{(a-b)\cos\theta_1 \sin(\theta_2-\theta)}{\sin(\theta_2-\theta_1)\cos\theta} \\ r = \dfrac{(a-b)\cos\theta_2 \cos\theta_1}{\sin(\theta_2-\theta_1)\cos\theta} \end{cases} \tag{5}$$

where Y is the distance between the micro-unit body and the right boundary of the pillar; θ_1 and θ_2 are the vertical angles formed by stress point A and the two boundaries of the pillar, respectively; a and b are the distances between the origin of coordinates and the right and the left boundaries of the pillar, respectively.

Based on the relationship ($y=Y+b$) between the y coordinate of the concentrated force point in the pillar's micro-unit body and distance Y from the concentrated force point to the right boundary of the pillars. Whereby the linear pillar loading can be expressed as follows:

$$q(y) = q_1 + q_2 \tag{6}$$

where $q_1=\alpha Y$ and $q_2=\alpha b+\beta$.

By combining equations (3)～(6), and taking the expression q_1 as a reference, the floor strata stress under the effect of pure linear loading q_1 is obtained as follows:

$$\begin{cases} \sigma_{1x} = -\dfrac{\alpha}{\pi}\dfrac{(a-b)\cos\theta_1}{\sin(\theta_2-\theta_1)}\left[(\theta_2-\theta_1)\sin\theta_2 - \sin\theta_1\sin(\theta_2-\theta_1)\right] \\ \sigma_{1y} = -\dfrac{\alpha}{\pi}\dfrac{(a-b)\cos\theta_1}{\sin(\theta_2-\theta_1)}\left[(\theta_2-\theta_1)\sin\theta_2 + \sin\theta_1\sin(\theta_2-\theta_1) - 2\cos\theta_2\ln\left(|\cos\theta_1|/|\cos\theta_2|\right)\right] \\ \tau_{1xy} = -\dfrac{\alpha}{\pi}\dfrac{(a-b)\cos\theta_1}{\sin(\theta_2-\theta_1)}\left[\sin\theta_2 - \sin\theta_1\cos(\theta_2-\theta_1) - (\theta_2-\theta_1)\cos\theta_2\right] \end{cases} \tag{7}$$

where σ_{1x}, σ_{1y}, and τ_{1xy} are the respective floor stress components under the q_1 loading effect.

The stress solution under uniform loading condition q_2 is as follows (Yang W et al., 2012):

$$\begin{cases} \sigma_{2x} = -\dfrac{q_2}{2\pi}\left[2(\theta_2-\theta_1) + (\sin 2\theta_2 - \sin 2\theta_1)\right] \\ \sigma_{2y} = -\dfrac{q_2}{2\pi}\left[2(\theta_2-\theta_1) - (\sin 2\theta_2 - \sin 2\theta_1)\right] \\ \tau_{2xy} = \dfrac{q_2}{2\pi}(\cos 2\theta_2 - \cos 2\theta_1) \end{cases} \tag{8}$$

where σ_{2x}, σ_{2y}, τ_{2xy} are the floor strata stress components under the q_2 loading effect.

By combining equations (6)～(8), the floor strata stress under the linear loading is obtained as follows:

$$\begin{cases} \sigma_x = \sigma_{1x} + \sigma_{2x} \\ \sigma_y = \sigma_{1y} + \sigma_{2y} \\ \tau_{xy} = \tau_{1xy} + \tau_{2xy} \end{cases} \tag{9}$$

As indicated by equations (7)～(9), the stress distribution in floor strata under the linear loading condition depends mainly on linear loading characteristics of the coal pillars and the stress position. The stress at different positions under the pillars are different, and the stress at the same position would also increase linearly with the increase of load borne by the pillars.

It can also be seen from Fig.1 that the vertical angle between stress point A in floor strata and the pillar boundaries, and the coordinates of point A satisfy the following relationship:

$$\theta_1 = \arctan\frac{y_A - a}{x_A},\ \theta_2 = \arctan\frac{y_A - b}{x_A} \tag{10}$$

where x_A and y_A are ordinate and abscissa of a stress point A in floor strata, respectively.

A case study of the effect of coal pillars in the goaf areas

Major coal occurrences in the Datong mining area of Shanxi are Jurassic and Carboniferous seams. With the Jurassic seams almost completely excavated, the thick and extra-thick Carboniferous seams are now the primary seams being mined. Between the two types of seams, there are layers of fine-grained sandstone, coal,

siltstone, medium-grained sandstone, conglomerate and sandy mudstone. The distance between two types of seams aregenerally 150~200 m, for which sandy formations account 90 % to 95 %, while mudstone and coal account 5 % to 10 %. Above the 8104 working face of Carboniferous seam are the 8202~8210 working faces of Jurassic seam, which have been fully excavated during 1981 to 1988. The coal and rock physical and mechanical parameters as shown in Tab.1.

Tab. 1. Coal and rock physical and mechanical parameters.

No.	Lithology	Bulk modulus [GPa]	Shear modulus [GPa]	Density [kg/m³]	Tensile strength [MPa]	Cohesion [MPa]	Angle of internal friction [°]
14	**Fine-grained sandstone**	10.6	11.5	2534	7.8	15.7	47.0
13	**Sandy mudstone**	13.9	9.6	2595	5.2	5.5	33.0
12	**Jurassic coal seam**	2.6	1.1	1426	2.6	9.5	30.0
11	**Fine-grained sandstone**	10.6	11.5	2534	7.8	15.7	47.0
10	**Medium-grained sandstone**	7.2	6.1	2526	7.0	6.8	31.0
9	**Medium-grained siltstone**	11.7	7.4	2575	7.0	9.6	37.0
8	**Medium-grained sandstone**	7.2	6.1	2526	7.0	6.8	31.0
7	**Sandy mudstone**	13.9	9.6	2595	5.2	5.5	33.0
6	**Mudstone**	14.3	8.6	2654	4.8	4.9	34.0
5	**Siltstone**	12.3	10.0	2747	5.6	8.5	30.9
4	**Magmatic rock**	16.9	18.5	2747	10.7	16.5	50.0
3	**Carbonaceous mudstone**	13.9	9.6	2728	4.0	5.5	33.0
2	**Carboniferous coal seam**	2.6	1.1	1426	2.6	9.5	30.0
1	**Kaolin**	12.3	10.0	2595	5.2	8.5	30.9

The 8104 working face is advanced in a direction perpendicular to the advancing direction in Jurassic coal seam. The open-off cut of 8104 working face is below boundary pillars of the Jurassic seam and about 655 m away from the edge of the gob of 8202 working face. The stratigraphic relationship between the two seams is as presented in Fig.2.

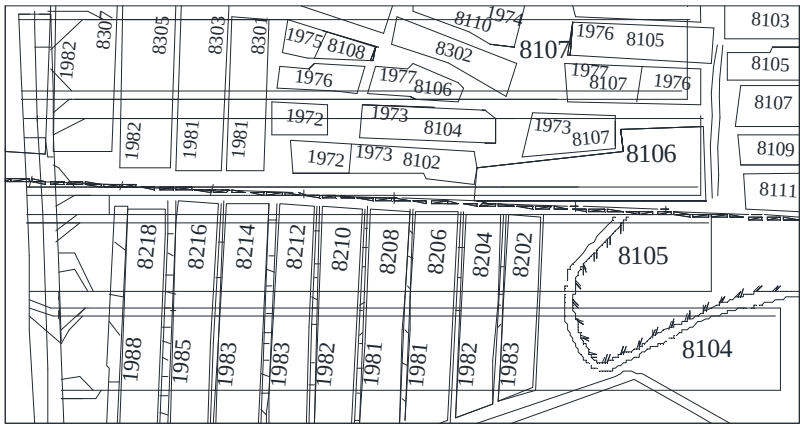

Fig. 2. The relationship between working faces in coal seams of two geological ages.

The roof strata movement in Jurassic coal seam has basically stabilized after a long period of motion adjustment. The coal pillars left behind in the goaf areas as the arch foot continue to bear the weight from the overlying strata, resulting in the relatively high-stress concentration areas underneath the coal pillars left in the Jurassic coal goaf. With the mining of the Carboniferous coal seam below, the effects of the large goafs are likely to be spread to the already stabilized Jurassic overlying roof structure. The overburden structures of these two seams are interconnected, which can cause the sudden release of the highly elastic energy stored in stress concentrated areas below the pillars, threatening the safety and effective production at the lower coal seam (Yu B, 2014). The characteristics of the overlying rock structure of the dual coal seams in the Tongxin Coalmine are shown in Fig. 3.

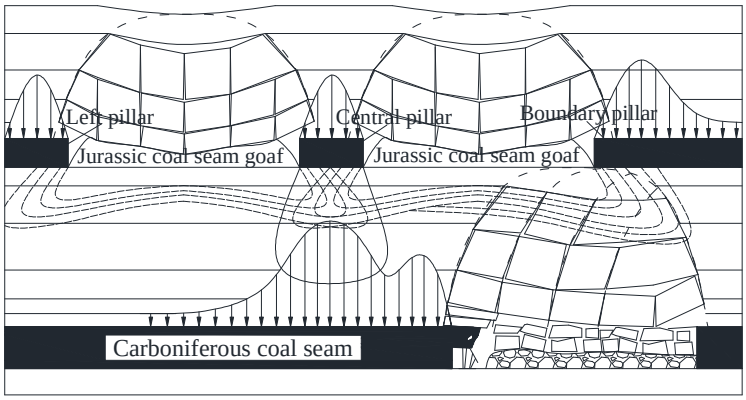

Fig. 3. Tongxin Coalmine's overburden structure at the dual coal seams.

After Jurassic coal seam was mined, the roof structure has stabilized after a long period of time. The caving gangues have stabilized into a uniform loading state while the loading stress on the coal pillars is relatively concentrated (Liu CY et al., 2007; Xie GX et al., 2006; Yu B, 2014). Considering the facts that the coal pillars are generally small in height and exposed to prolonged loading and that destabilization and elastic deformation in the goaf-sides are liable to occur, bilinear loading was adopted to approximate the actual loading curve of the pillars. Meanwhile, the model for the stress in floor strata of the Jurassic coal seam was constructed through a comparative analysis of the characteristics of floor strata stress under the uniform loading condition, as shown in Fig.4.

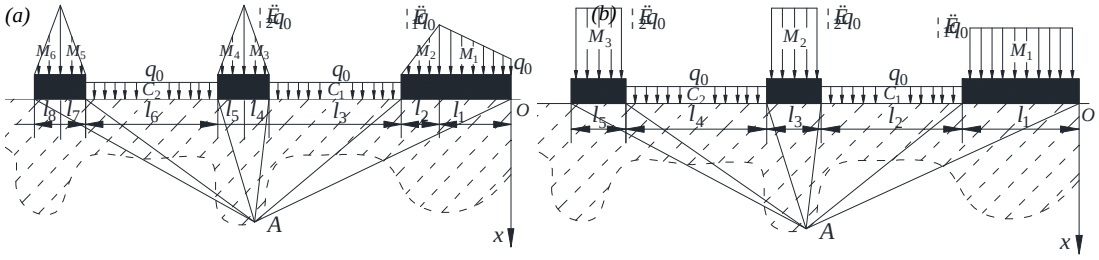

Fig. 4. Model of stress in floor strata below Jurassic coal seam: (a) linear loading; (b) uniform loading.

The coordinate origin is set at the right border of the boundary pillar; C_1 and C_2 are the goaf areas of 8202 and 8204 working faces at the Jurassic coal seam, respectively, q_0 is the in-situ stress exerting on gangues, and $l_3$and l_6 are the widths of the goafs, respectively. Within the limit from the highest stress point of the pillar to the two boundaries of the pillar, the boundary pillar in 8202 working face of Jurassic seam is divided into two sections: M_1 and M_2, and the maximum stress of boundary pillar is $\lambda_1 q_0$, where λ_1 is the stress concentration coefficient, and the widths of two sections of the boundary pillar are l_1 and l_2, respectively. Similarly, pillars in each goaf section were divided into sections from M_3 to M_6, and due to structural symmetry, the highest coal pillar stress is taken as $\lambda_2 q_0$, the stress concentration coefficient as λ_2, and the widths of different sections of section coal pillars are l_4, l_5, l_7 and l_8, respectively. Similarly, the states of coal pillars under uniform loads are also divided into different sections.

In accordance with the coal reserves and the stress characteristics of the Jurassic coal seam at Datong coal mining region: the working faces have an average length of 150 m, the section pillars size are 20 m and the boundary pillar size is 80 m, the in-situ stress is 6.5 MPa, the boundary and section pillars' stress concentration coefficient is 1.6 and 2.3, respectively (Yu B et al., 2013). The stress distribution characteristics of floor strata under the uniform and bilinear loading condition were obtained by using the calculation software of MATLAB, as shown in Fig. 5.

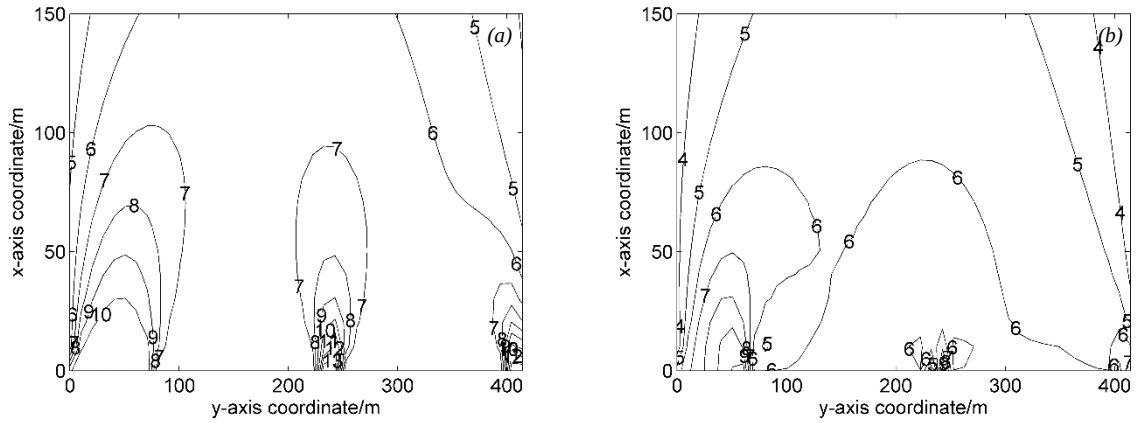

Fig. 5. Distribution characteristics of vertical stress in floor strata: (a) uniform loading; (b) bilinear loading.

Fig. 5 (a) shows the vertical stress distribution in floor strata below the Jurassic coal seam when the goaf pillars are under uniform loading condition. The vertical stress is mainly concentrated beneath the corresponding pillars, and the depth of the vertical stress concentration zone affected by and beneath the boundary pillar is about 70 m, the horizontal extent affected and the width designed for the boundary pillar are similar at about 60 ~ 80 m, and the maximum vertical stress is 10.5 MPa or so. The depth of the stress concentration zone affected by section coal pillars is about 50 m, the horizontal extent affected is about 20 ~ 30 m, and the maximum stress in the stress concentration zone is about 13.9 MPa, about 1.3 times as much as the maximum stress of the boundary pillar.

Fig. 5 (b) presents the vertical stress distribution in floor strata under bilinear loading condition. The depth of the stress concentration zone affected by and beneath the boundary and section pillars is about 70 m and 30 m, respectively; the horizontal extent affected is about 60 m and 20 m, respectively; and the maximum vertical stress is all about 10.5 MPa.

Thus, under both loading conditions, the depth of the vertical stress concentration zone in floor strata beneath the boundary pillar and the maximum stress value were basically the same, but under the uniform loading, the width of the stress affected zone was about 1.0 to 1.3 times as much as that bilinear loading condition. When section coal pillars are under uniform loading, the depth, width and maximum stress of the vertical stress affected zone were 1.6 times, 1.0 to 1.5 times and 1.3 times, respectively, as much as those bilinear loading condition.

Similarly, when the boundary pillars are under uniform loading, the depth, width and maximum stress of the area affected by the horizontal stress in floor strata are 2.0 times, 1.3 times and 1.1 times, respectively, and affected by the energy density are 1.3 times, 1.2 times, and 1.1 times, respectively, as much as those bilinear loading condition.When the section coal pillars are under uniform loading, the depth, width and maximum stress of the area affected by the horizontal stress in floor strata are 2.0 times, 1.0 to 2.0 times and 1.4 times, and affected by the energy density are 2.0 times, 1.0 to 2.0 times and 1.8 times, respectively, as much as a bilinear loading condition.

In order to understand the interactions between the multiple coal pillars in the goaf areas, the vertical stress distributions of the individual and integrated impacts of the coal pillars in Jurassic coal seam goaf areas are shown in Fig. 6.

The black curve with some dots represent integrated impacts of the coal pillars in the goaf areas; the dot-dash and the dashed line represent the individual impacts of the central and left section pillars, and the black curve represents the individualimpacts of the boundary pillar. It can be observed that, as the vertical distance from the pillars increases, the width of a single pillar-affected zone increases, but the vertical stress peak value decreases.

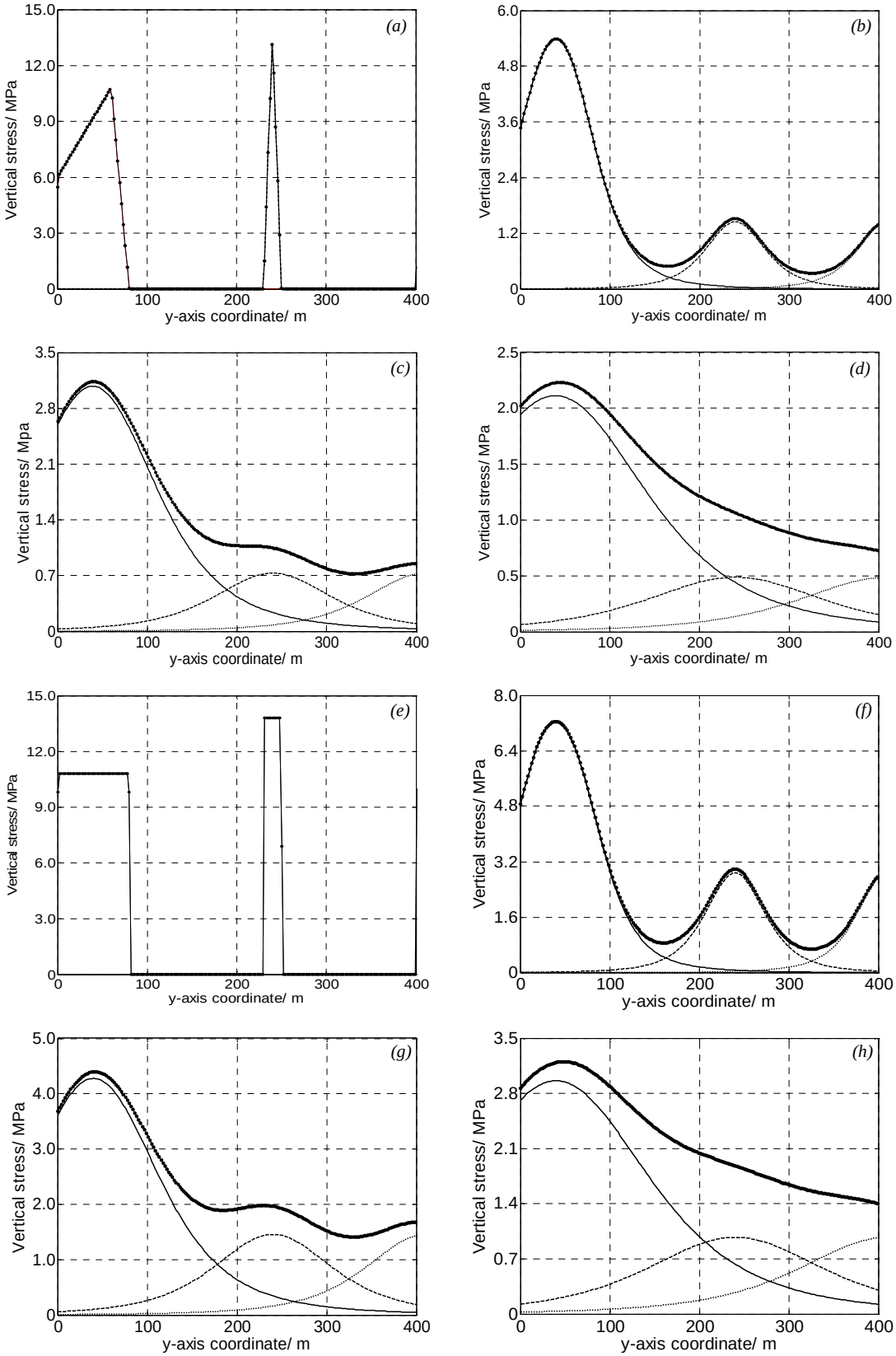

Fig. 6. Vertical stress distributions in floor strata under two types of loading condition: group (a) ~ (d) and group (e) ~ (h) are vertical stress distributions at different distances (0m, 60m, 120m, 180m, respectively) from the bottom of the pillar under the bilinear and uniform loading condition.

Assuming the width of the vertical stress concentration zone is 0.5 times the peak stress value, the characteristics of the vertical stress distribution under two types of loading condition are shown in Fig. 7.

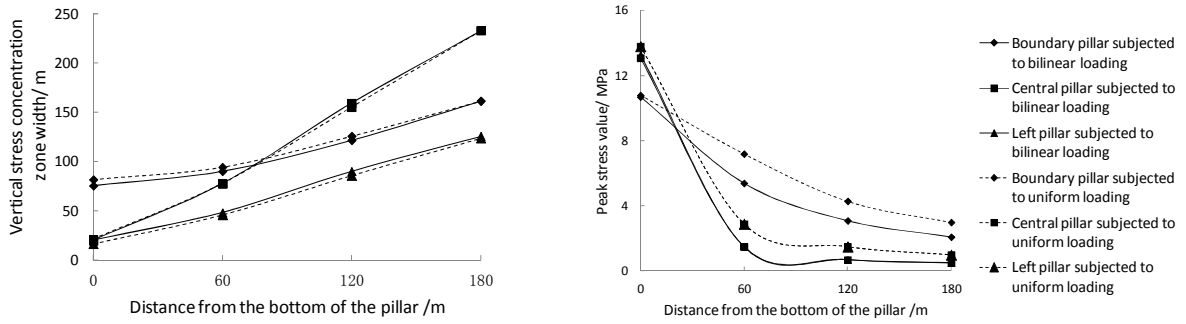

Fig. 7. Vertical stress distribution characteristics.

At the same position of the floor strata, the vertical stress under the uniform loading is approximately 1.0 to 2.0 times as much as that bilinear loading condition.

The width of the area affected by the vertical stress at the pillar bottom is relatively large under the uniform loading, which is about 1.1 times as much as that bilinear loading condition. When the distance is 60 ~ 180 m from the pillar bottom, the widths of the vertical stress affected areas under both loading conditions are basically the same.

When the distance from the bottom of the pillar is 0 ~ 60 m, the stress in floor strata is mainly from the overlying single pillar action, largely unaffected by other coal pillars in the goaf areas. When the distance is 120 m, the impacts from the multiple pillars increase, and the superposed vertical stress at the position corresponding to the peak value of the individual pillar impact increases by about 0.1 to 0.3 times. When the distance is 180 m, the integrated impacts from the multiple pillars are extremely significant, the superposed vertical stress at the corresponding position has increased by about 0.2 to 1.0 times.

Similarly, as the distance from the pillar bottom increases, affected by the spatial effect of the goaf areas, the floor strata below the goaf areas was subjected to larger lateral deformation, and the horizontal stress shifted to the sides of the goaf areas, resulting in the higher horizontal stress in floor strata. The horizontal stress distributions of the individual and integrated impacts of the pillars are shown as in Fig. 8.

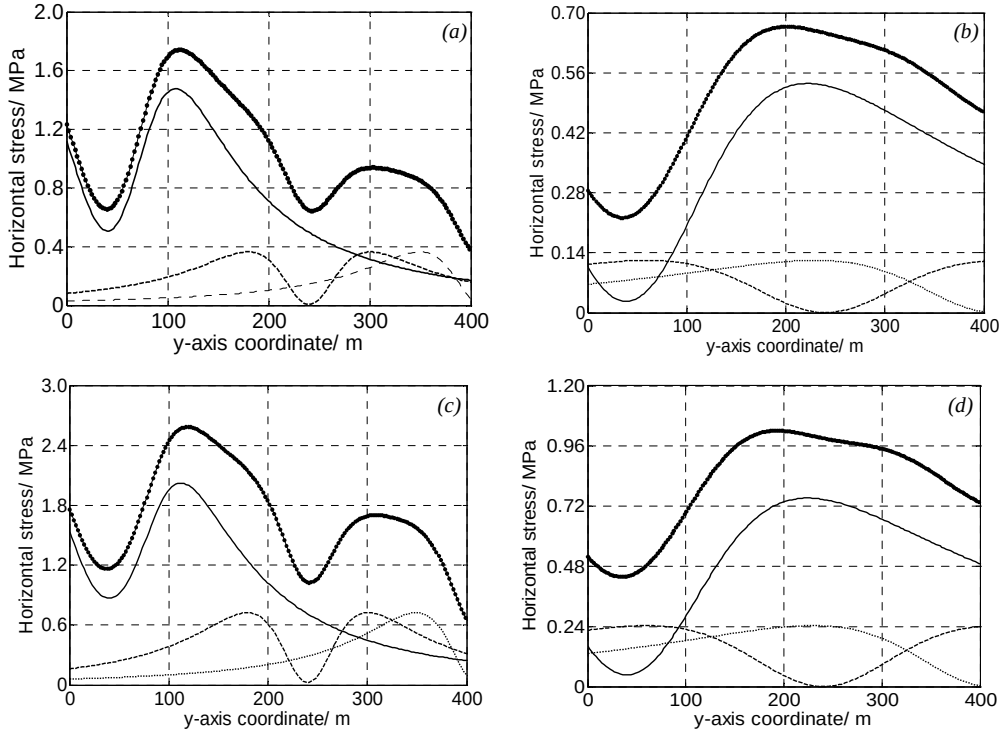

Fig. 8. Horizontal stress distribution in floor strata under two types of loading condition: group (a) ~ (b) and group (c) ~ (d) are horizontal stress distributions at different distances (60m, 180m, respectively) from the bottom of the pillar under the bilinear and uniform loading condition.

If 0.5 times of the horizontal peak stress value on the side of the goaf areas is taken as the boundary of the stress concentration area in floor strata, the effects on the horizontal stress in floor strata under the two loading conditions are as shown in Fig. 9.

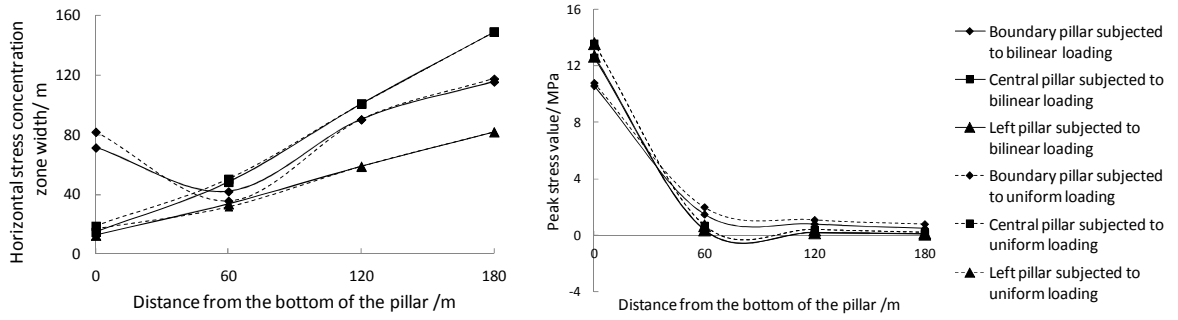

Fig. 9. Horizontal stress distribution characteristics.

The horizontal stress at the pillar bottom is more significantly affected by individual coal pillars while at other positions the integrated impacts between the multiple pillars are higher.

As the distance from the pillar bottom increases, the width of stress concentration area by a single pillar gradually increases, and the horizontal peak stress value also decreases. The horizontal stress and the width of the area at the bottom of the pillar under the uniform loading are about 1.3 times and 1.1 to 1.3 times as much as that bilinear loading condition.

When the distance is 60 ~ 180 m from the pillar bottom, the horizontal stress in floor strata below the coal pillar under the bilinear loading is generally higher than that uniform loading condition; the increase is about 1.8 to 3.0 times in the same position. The widths of the stress concentration area under both loading conditions are basically the same, and the impacts from the multiple pillars are more significant, the superposed horizontal stress at the position corresponding to the peak stress value under the impact of the original single pillar increases by about 0.1 to 0.8 times.

Similar to the distribution characteristics of the vertical stress, as the distance from the coal pillar bottom increases, the width of the energy density area under a single pillar increases, and the peak energy density value decreases. If 0.5 times of the peak energy density value is taken as the boundary of the energyaffected area, the characteristics of the energyaffected area under the two loading conditions are shown in Fig. 10.

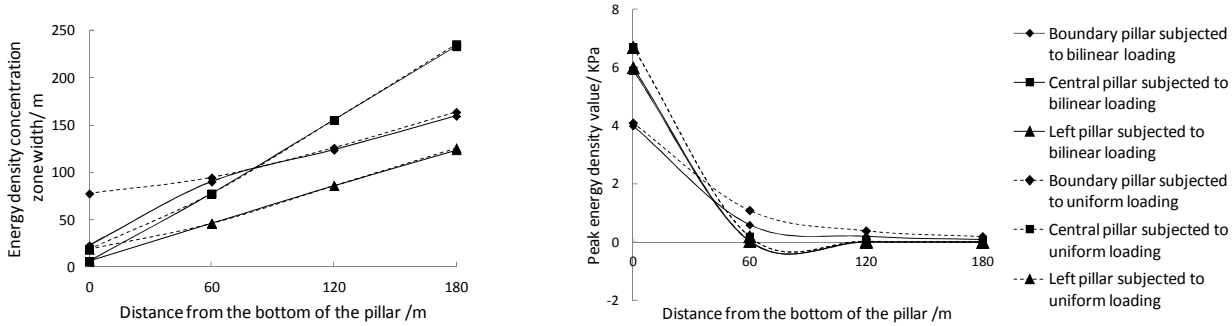

Fig. 10. Energy density distribution characteristics.

Under uniform loading condition, at the same position below the boundary and section pillars, the energy density is about 1.0 to 2.2 times and 1.1 to 5.0 times respectively, as much as that bilinear loading.

The width of energyaffected area at the pillar bottom is 3.0 to 3.4 times under uniform loading as much as the bilinear loading condition. When the distance is 60 ~ 180 m from the pillar bottom, the widths of energyaffected area under the two loading conditions are basically the same.

When the distance is 0 ~ 60 m, the energy in floor strata is mainly from the overlying single pillar action. When the distance is 120 ~ 180m, the multiple pillars have impacts on each other, and the total sum of the energy at the same position in floor strata is approximately 1.0 to 2.7 times as much as the maximum energy value from the single pillar action.

The previous analysis showed that under the same peak loading and elevation position, the distribution forms of stress and energy was the same, but the effects of the uniform loading on stress and energy value were greater than the bilinear loading condition. The distribution of stress in the floor under the coal pillars under the same conditionswas calculated from the physicomechanical parameters shown in Table 1 using the UDEC

software. Moreover, the increased stress coefficient was defined as the ratio of current stress to the initial stress at a point. Then the distributions of stress in the floor under the coal pillars in the goafs in the Jurassic seam and the increased stress coefficient were obtained, as shown in Fig. 11.

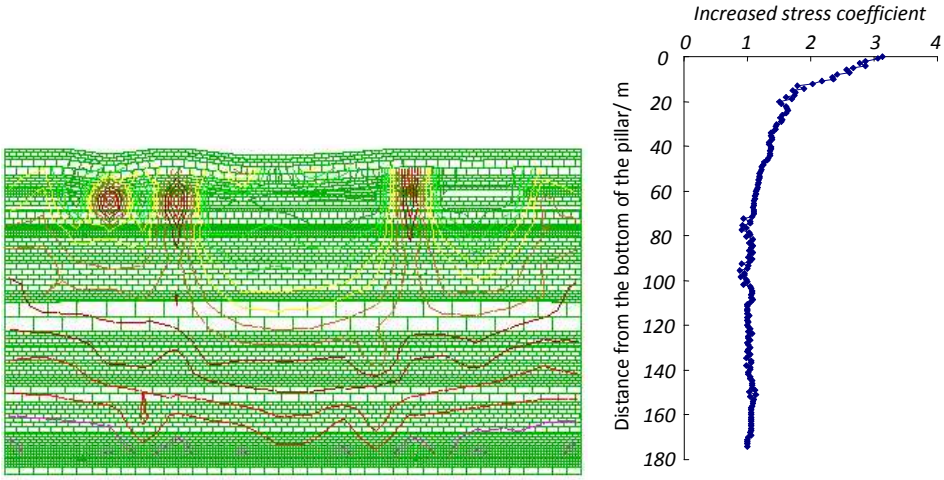

Fig. 11. The distributions of stress and increased stress coefficient in floor under coal pillars.

It is observed that the distribution patterns of floor stress under the coal pillars left behind in the goafs in the Jurassic coal seam are largely consistent with the theoretical results presented in Fig.5. In addition, the relationship between the increased stress coefficient and depth indicates that the depth of the vertical stress concentration zone affected by and beneath the pillars is about 60 ~ 70m,consistent with the results of theoretical analysis. This demonstrated that this theoretical method for calculating the stress in the floor beneath pillars and its scope of influence is accurate and applicable. To achieve more accurate stress calculation, the characteristics of stress and energy distribution were obtained by segmented straightening approximation of the actual loading curve, in this way, the approximation solution of the stress in floor strata under the actual loading conditions can be obtained. Fig.12 shows the effects of approximation when the loading stress curve uses three and eight linear loading.

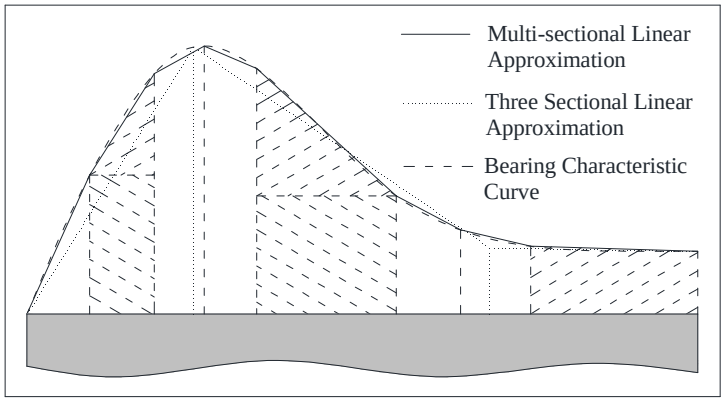

Fig. 12. Effects of segmented straightening of loading characteristic curves.

As indicated in Fig.12, when the approximation is made towards the actual loading curve of the coal pillars in the goaf areas through segmented linear loading, the more segments there are, the more accurate the solution for the stress in floor strata is.

Conclusions

Through a theoretical analysis, mathematic expressions of stress in floor strata when the coal pillars are under arbitrary linear loading conditions were established. By segmented straightening approximation of the actual loading curve and finding segmented solutions, the characteristics of stress and energy distribution in floor strata affected by the coal pillars left in the goaf areas were obtained.

When the coal pillars left in the goaf areas were under the bilinear and uniform loading conditions, the stress and energy distribution in the floor strata presented different characteristics. Under the same peak

loading and elevation position, the distribution forms of stress and energy were the same, but the effect of the uniform loading on stress and energy value in floor strata were greater than the bilinear loading condition.

The vertical stress and the energy density within a certain critical distance from the bottom of the pillar were mainly affected by the overlying single pillar action. However, beyond this critical distance, the vertical stress and the energy density in floor strata were gradually affected by the interactions between the multiple pillars, and the horizontal stress was more vulnerable to the interactions of the multiple pillars under different loading conditions.

***Acknowledgment**: This work was supported by China Postdoctoral Science Foundation Project (2015M581896), Fundamental Research Funds Project (2014ZDPY21) for the Central Universities, and Priority Academic Program Development of Jiangsu Higher Education Institutions.*

References

Gao MS, Dou LM, Zhang N.: Cusp catastrophic model for instability of coal pillar burst damage and analysis of its application, In: *Journal of China University of Mining & Technology, Vol.34, No.4, 2005, pp.433-437*.

Gong KY, Shan CJ.: Ground pressure appeared mechanism and control of roadway under the coal pillar, In: *Ground Pressure and Strata Control, No.4, 2001, pp.20-21*.

Gong PL, Jin ZM.: Mechanical model study on roof control for fully-mechanized coal face with large mining height, In: *Chinese Journal of Rock Mechanics and Engineering, Vol.27, No.1, 2008, pp. 193-198*.

Hao HJ, Wu J, Zhang Y, Yuan ZB.: The balance structure of main roof and its action to immediate roof inlarge cutting height workface, In: *Journal of China Coal Society, Vol.29, No.2, 2004, pp.137-141*.

Liu BC, Shen HQ.: The mathematical model and solution for optimization of coal pillar for preventing building, In*: Journal of China Coal Society, Vol.13, No.3, 1988, pp.18-25*.

Liu CY, Huang BX, Meng XJ, Yang PJ, Chen LG.: Research on abutment pressure distribution law of over length isolated fully-mechanized top coal caving face,In:*Chinese Journal of Rock Mechanics and Engineering, Vol.26, No.1, 2007, pp.2671-2676*.

Meng D, Wang JC, Wang JX.: Mechanism on the failure and caving of roof strata in pillar and house mining, In: *Journal of China Coal Society, Vol.32, No.6, 2007, pp.577-580*.

Tu SH, Wang FT, Dou FJ, Yuan Y, Lu Y.: Fully mechanized top coal caving: underground stress at gateways under barrier pillars of an upper coal seam, In: *Journal of China University of Mining & Technology, Vol.39, No.1, 2010, pp.1-5*.

Wang WJ, Hou CJ.: Stability analysis of coal pillar and immediate bottom of extraction opening, In: *Rock and Soil Mechanics, Vol.24, No.1, 2003, pp.75-78*.

Xie GX, Yang K, Liu QM.: Study on distribution laws of stress in inclined coal pillar for fully-mechanized top-coal caving face, In: Chinese *Journal of Rock Mechanics and Engineering, Vol.25, No.3, 2006, pp.545-549*.

Xu ZL.: Elasticity, *Beijing, Higher Education Press, 2006.*

Yang JX, Liu CY, Yang Y, Li JW: Study of the bearing mechanism of the coal roof and the dimension selection of the room and pillar in the shallow and close distance coal seam, In: *Journal of China University of Mining & Technology, Vol.42, No.2, 2013, pp.161-168.*

Yang W, Liu CY, Huang BX, Yang Y.: Determination on reasonable malposition of combined mining in close-distance coal seams, In: *Journal of Mining & Safety Engineering, Vol.29, No.1, 2012, pp.101-105*.

Yu B.: Study on strong pressure behavior mechanism and roof control of fully mechanized top coal caving in extra thickness seam in datong coal mine, *Xuzhou, China University of Mining & Technology, 2014*.

Yu B, Liu CY, Yang JX, Liu JR.: Research on the fracture instability and its control technique of hard and thick roof, In: *Journal of China University of Mining & Technology, Vol.42, No.3, 2013, pp.342-348.*